An inkjet vision measurement technique for high-frequency jetting

Kye-Si Kwon, Min-Hyuck Jang, Ha Yeong Park, and Hyun-Seok Ko

Citation: Review of Scientific Instruments **85**, 065101 (2014); doi: 10.1063/1.4879824
View online: http://dx.doi.org/10.1063/1.4879824
View Table of Contents: http://scitation.aip.org/content/aip/journal/rsi/85/6?ver=pdfcov
Published by the AIP Publishing

An inkjet vision measurement technique for high-frequency jetting

Kye-Si Kwon,[1,a)] Min-Hyuck Jang,[1] Ha Yeong Park,[1] and Hyun-Seok Ko[2]
[1]*Department of Mechanical Engineering, Soonchunhyang University 22, Soonchunhyang-Ro, Shinchang, Asan Chungnam 336-745, South Korea*
[2]*Department of Electrical and Robot Engineering, Soonchunhyang University, 22, Soonchunhyang-Ro, Shinchang, Asan Chungnam 336-745, South Korea*

(Received 11 February 2014; accepted 13 May 2014; published online 3 June 2014)

Inkjet technology has been used as manufacturing a tool for printed electronics. To increase the productivity, the jetting frequency needs to be increased. When using high-frequency jetting, the printed pattern quality could be non-uniform since the jetting performance characteristics including the jetting speed and droplet volume could vary significantly with increases in jet frequency. Therefore, high-frequency jetting behavior must be evaluated properly for improvement. However, it is difficult to measure high-frequency jetting behavior using previous vision analysis methods, because subsequent droplets are close or even merged. In this paper, we present vision measurement techniques to evaluate the drop formation of high-frequency jetting. The proposed method is based on tracking target droplets such that subsequent droplets can be excluded in the image analysis by focusing on the target droplet. Finally, a frequency sweeping method for jetting speed and droplet volume is presented to understand the overall jetting frequency effects on jetting performance. © *2014 AIP Publishing LLC*. [http://dx.doi.org/10.1063/1.4879824]

I. INTRODUCTION

The application of inkjet technology has been broadening from home printers to manufacturing tools. To use piezo inkjets as a manufacturing tool for printed electronics, the productivity and reliability of the technology have become two key issues. To increase the productivity, high-frequency jetting is required. In high-frequency jetting, subsequent droplets could be ejected before the pressure wave from the previous drop has sufficiently decayed inside the inkjet head, which will affect jetting behavior.[1] To ensure printing uniformity, high-frequency jetting behavior must be evaluated prior to any improvement.

Recently, the use of pressure wave signals measured by piezo self-sensing was proposed to evaluate the waveform for high-frequency jetting performance.[1] However, the jetting speed and droplet volume behavior are difficult to understand since the amplitude of the self-sensing signal may not be directly related to the jetting behavior. So, in this study, vision analysis methods are mainly discussed, because the high frequency effects on printing quality can be easily understood by visual means.

For inkjet vision analysis, images from charge-coupled device (CCD) cameras are widely used to measure droplet jetting speed and droplet volume.[2,3] By using light-emitting diode (LED) light synchronized to the firing signal, droplet images appear to be frozen in the acquired CCD camera image. Then, image processing techniques are used to measure jetting speed and droplet volume.[2–4] However, the jetting speed varies significantly during drop formation. As a result, the jetting speed measured using previous methods in Refs. 3 and 4 can differ according to the selection of the two timings or measurement location.

Recently, the instantaneous jetting speed curve was proposed to overcome the shortcomings of jetting speed measurement based on two timings.[5] The use of instantaneous jetting speed curve has advantages because jetting speed variation during drop formation can be understood. Also, the relative jetting speed of satellites with respect to the main droplet can be measured during drop formation. However, it may have limitations in measuring high-frequency jetting behavior, because the result of image analysis might be very complicated to understand due to the many subsequent droplets in the acquired images. Furthermore, the measurement of drop formation is made even more difficult by the subsequent droplets possibly merging with the droplet of interest.

To authors' best knowledge, there are no standardized methods and few studies on vision measurement techniques to evaluate the jetting performance of such complex high-frequency jetting behavior. The inkjet industry seems to have their own technique to measure high-frequency jetting behavior, but the measured results are likely to differ according to individual measurement methods.

In this study, to measure high-frequency jetting behavior effectively, we propose a measurement method based on tracking of a main droplet. Also, the use of a variable ROI (region of interest), of which the size and location is re-defined in each sequential image, is proposed to focus image analysis on tracked target droplets while excluding image analysis of the other subsequent droplets.

As an application of the high-frequency jetting measurement, a frequency sweep method for jetting speed and droplet volume is discussed to effectively evaluate frequency effects on jetting.

[a)]Author to whom correspondence should be addressed. Electronic mail: kskwon@sch.ac.kr. Telephone: Int+ 82-41-530-1670. Fax: Int +82-41-530-1550. URL: http://inkjet.sch.ac.kr/.

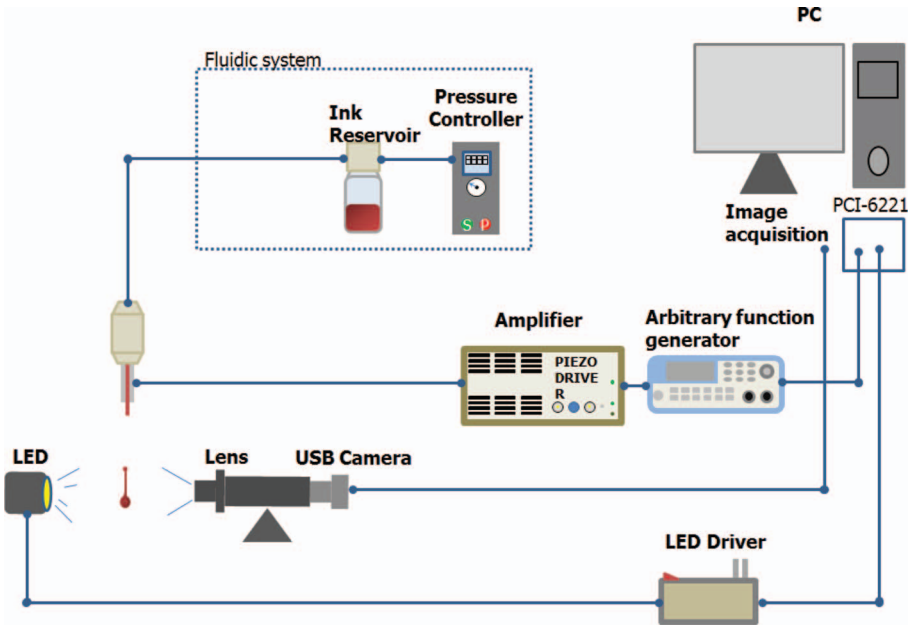

FIG. 1. Drop watcher system.

II. MEASURING DROP FORMATION OF HIGH FREQUENCY JETTING

In this section, a new vision-based method for measuring high-frequency jetting performance is proposed. To implement and verify the proposed measurement method, the laboratory-developed strobe LED system shown in Fig. 1 was used.

A single nozzle head (MJ-AT, Microfab) was used as the jetting device. The nozzle diameter of the printhead used for the experiment was 50 μm. Standard inkjet ink (XL-30, Dimatix) was used as a jetting fluid. To visualize jetting images, a CCD camera (STC-TC202USB, Sentech, Japan) was used for jet image acquisition. An adjustable zoom lens (ML-Z07545, MORITEX, Japan) and a lens adaptor (ML-Z20, MORITEX, Japan) were used to acquire magnified images of the inkjet behavior. To obtain frozen jetting images, LED lights were synchronized with jet triggers.

Two digital pulse trains from a counter board (PCI-6221, NI) were used for the synchronization, as shown in Fig. 2. The first digital pulse train is used as a trigger signal to generate the pulse voltage. The second pulse train is used to control the LED light. The second pulse is triggered from the first pulse. The trigger delay time between the first pulse and second pulse is adjusted so that the jet image at the delayed time can appear to be frozen. The details of the experimental setup can be referenced in a previous study.[5]

To obtain proper jetting, the shape of the pulse voltage should be optimized. The typical voltage waveform shown in Fig. 3 was used for jetting. The method for determining waveform parameters was discussed in detail in Ref. 6. In this study, to obtain the jetting conditions for measurement, the rising, falling, dwell time, and the voltage amplitude of the waveform were set to 6 μs, 6 μs, 20 μs, and 60 V, respectively. The total waveform length is 32 μs. If we only consider the waveform length, the maximum jetting frequency would be about 31 kHz (= 1/32 μs). It has been known that the pressure wave inside an inkjet head accounts for jetting, and the residual pressure wave after jetting should decay prior to the next jetting. This process could take some time. As a result, the usable frequency could be far less than the theoretical frequency limit of 31 kHz.

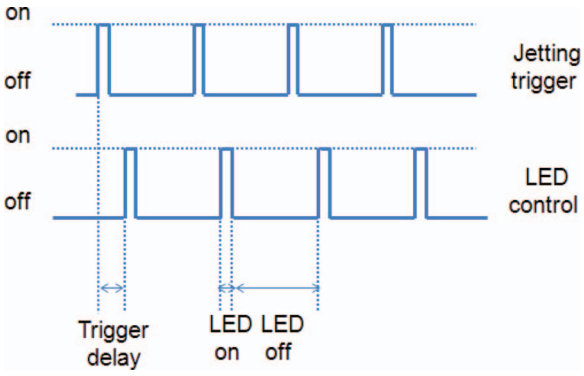

FIG. 2. Strobe LED control.

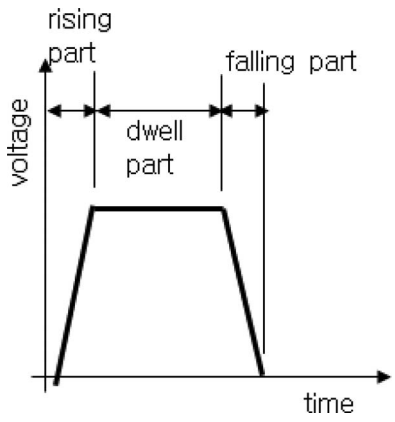

FIG. 3. Typical waveform voltage for jetting.

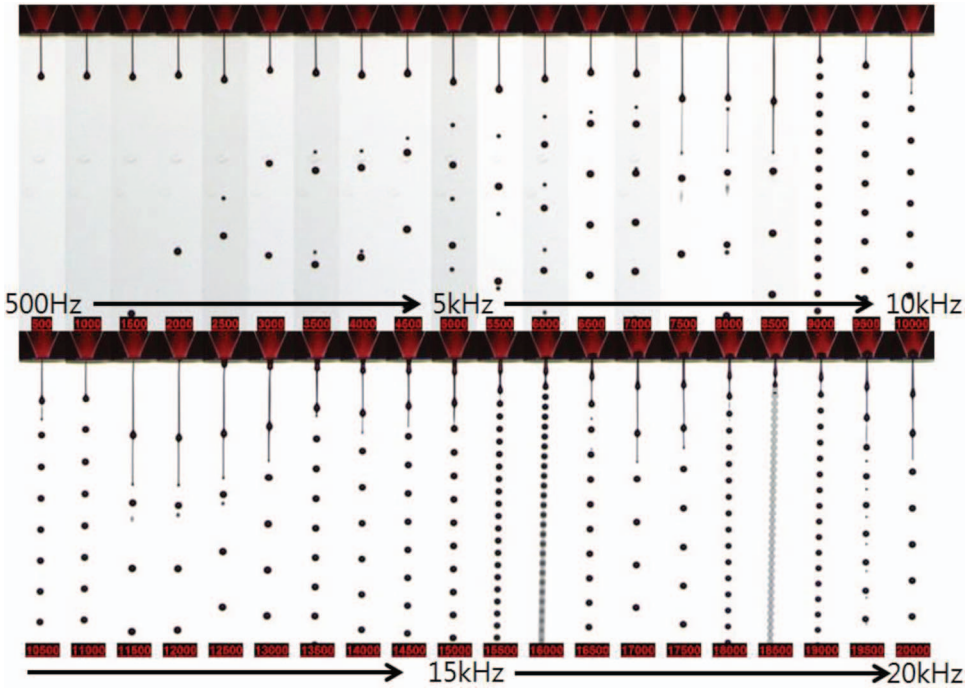

FIG. 4. Jetting frequency effects at 70 μs.

To obtain high-quality printing results using high-frequency jetting, the jetting behavior including the jetting speed and droplet volume should remain unaffected compared to nominal low-frequency jetting.

To illustrate frequency effects on jetting, jetting images of different frequencies ranging from 1.5 kHz to 20 kHz, are shown in Fig. 4. The same trigger delay of 70 μs for LED light with respect to the jetting trigger signal was used so that jetting images can be compared at the same time. As shown in Fig. 4, the droplet jetting behavior varies significantly according to jetting frequency.

At low frequencies such as 1 kHz, the jetted droplet of interest can easily be separated from other subsequent droplets for droplet vision analysis. However, at 7.5 kHz or higher jetting frequency, the jetting behavior from a pulse voltage is difficult to analyze using conventional binary image analysis due to the many subsequent droplets in the acquired images.

For better understanding of high-frequency measurement issues, the jetting behavior at 7.5 kHz will be discussed in detail without loss of generality. The droplet of interest is indicated as D_n as shown in Fig. 5. The subscript n means the current droplet number and the previous and subsequent droplet can be denoted as $n-1$ and $n+1$, respectively.

Interestingly, at 7.5 kHz, two different ligaments from the previous droplet denoted as L_{n-1} and the current droplet ligament denoted as L_n are attached to the droplet (D_n) of interest. As a result, the merged droplets (L_{n-1}, D_n, L_n) are likely to be mistaken for one droplet with a long ligament when using the conventional binary image analysis. With low frequency jetting at less than 5 kHz, the ligament L_{n-1} from previous jetting, hardly merges with the current droplet, D_n.

To overcome such difficulties in measuring high-frequency jetting, we propose a new image analysis algorithm, which can focus on a droplet of interest excluding other subsequent droplets. The measurement algorithm consists of three steps: (1) a tracking algorithm for a target droplet, (2) defining the variable ROI based on the tracked target droplets at each sequential image, and (3) drop formation analysis and droplet volume measurement based on the variable ROI.

A. Tracking algorithm of a target droplet

To focus image analysis on a specific droplet of interest among many droplets, a method widely used for particle tracking in image analysis, is applied to inkjet measurement. To track the droplet of interest related to the jetting trigger signal, it is important to find the initial extruded droplet from the nozzle. As a first step, initial jetting images are scanned using edge detection techniques to identify and search for the first extruded droplet after a jetting trigger signal. For this purpose,

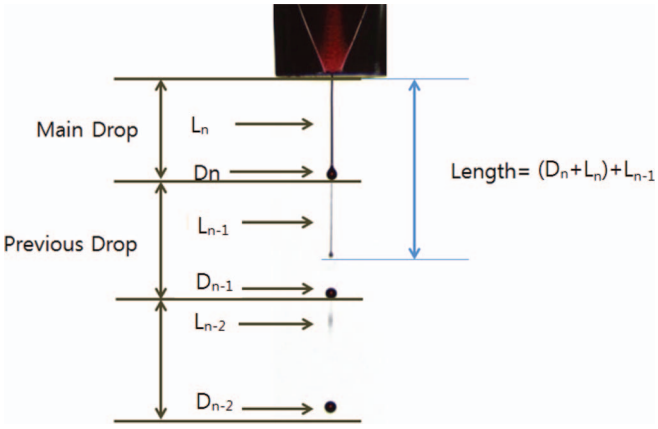

FIG. 5. High-frequency jetting behavior (7.5 kHz) at 70 μs.

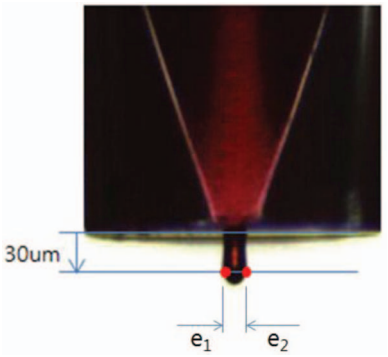

FIG. 6. Edge detection for detecting initial jetting.

the ROI (region of interest) line for edge detection is located 30 μm below the nozzle surface, as shown in Fig. 6.

The edge detection technique is widely used in image analysis to detect abrupt changes in image values along the ROI line. The inkjet jetting speed measurement using edge detection has been discussed in Ref. 3. In this study, the edge detection algorithm is used to detect the initial droplet by increasing the trigger delay time of the LED light with respect to the jetting trigger signal.

However, not all detected edges might be related to the initial droplet for tracking purposes. To identify an initial target droplet for tracking purposes and to ignore other detected edges such as those due to ligaments, the size of detected edges (e1 and e2 in Fig. 6(a)), defined by e = e2-e1, is compared with a threshold value. A threshold value of 30 μm was used to identify the initial extruded droplet for tracking.

The detected edges of droplets are ignored if the size of a detected droplet is less than the threshold value, because it is likely to be a ligament of previous droplets if the size is relatively small compared to the nozzle size. The threshold value should differ if an inkjet head with a different nozzle diameter is used. We used a nozzle with an inner diameter of 50 μm.

In some cases of high-frequency jetting, long ligaments may not be completely pinched off before the next droplet is jetted. For example, Fig. 7 shows some of the sequential images of the jetting behavior at 7.5 kHz. The pinch-off behavior of the ink droplet from the nozzle is marginally observed due to the long ligament and close subsequent droplets. Even in such complicated cases, the initial extruded droplet of interest for tracking can be successfully detected using the proposed edge detection technique.

Once the initial target droplet is detected, the track algorithm from NI Vision development module (NI) was used to track the droplet location from each sequential image. The

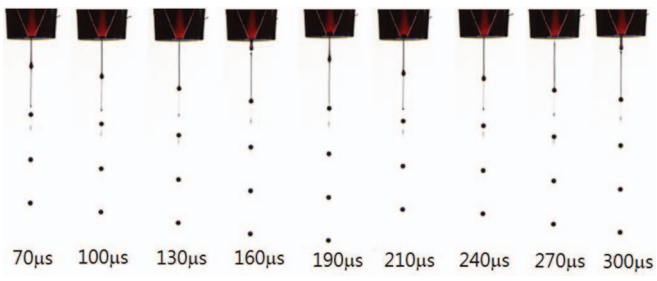

FIG. 7. Drop formation of typical high-frequency jetting (7.5 kHz).

track algorithm requires feature points (droplet shape) to track the feature shape. In inkjet applications, a spherical shape is searched for since the shape of the initial extruded droplets is similar to a sphere. Using the tracking algorithm, the target droplet is searched for and located from two successive image frames while ignoring many other droplets, which may appear in high-frequency jetting images.

However, inkjet droplets cannot be considered as merely a spherical particle because they can have long ligaments and satellites, which make the image analysis much more complicated than in conventional particle tracking algorithms.

B. Region of interest for image analysis

1. Fixed ROI

The tracking algorithm can be effectively used when the particle (point) behavior of a droplet is required. However, 2D area image analysis is required to include the satellite and ligament behavior rather than focusing on a single droplet as a particle. 2D ROI has been used[5,7,8] to measure the jetting behavior including ligament and satellites. However, the previous fixed ROI in Refs. 5, 7, and 8 for defining image processing area is likely to fail to analyze high-frequency jetting behavior of the target droplet due to the many other subsequent droplets.

For better understanding, the fixed ROI shown in Fig. 8(a) was used to obtain a drop formation curve for 7.5 kHz inkjet jetting. Since the jet behavior repeats with intervals of 133.3 μs (1/7.5 kHz), many drop formation curves for each subsequent droplet are obtained as shown in Fig. 8(b). Jetting behaviors including droplet location, ligament behavior and droplet volume per single jetting trigger are difficult to understand from the drop formation based on fixed ROI due to close subsequent droplets. Furthermore, the jetting behavior near the nozzle (0–0.5 mm) shows heavily merged behavior, and the analysis seems to be impossible.

2. Variable ROI

To overcome previous limitations, the variable ROI technique is proposed. The lower and upper locations of the ROI were re-defined in each sequential image to focus on the tracked target while excluding other droplets for droplet analysis.

Basically, two tracked subsequent droplets are used to define the boundary of ROI. However, only a single droplet or even no droplet is tracked in the initial stages. As a result, we need to consider the number of tracked droplets to define the variable ROI. This is a generalized method and can be applied to a broad range of frequencies since it can also be used for low-frequency jetting measurement.

(1) Stage 1: No tracked droplet

In the initial stage, the droplet of interest may not appear in the acquired image, because it will take time for the pressure wave of the ink inside the inkjet head to propagate before ink is ejected from the nozzle. In the case of no detected droplets, image analysis will be skipped, and the initial extruded target droplet will be found from the sequential images.

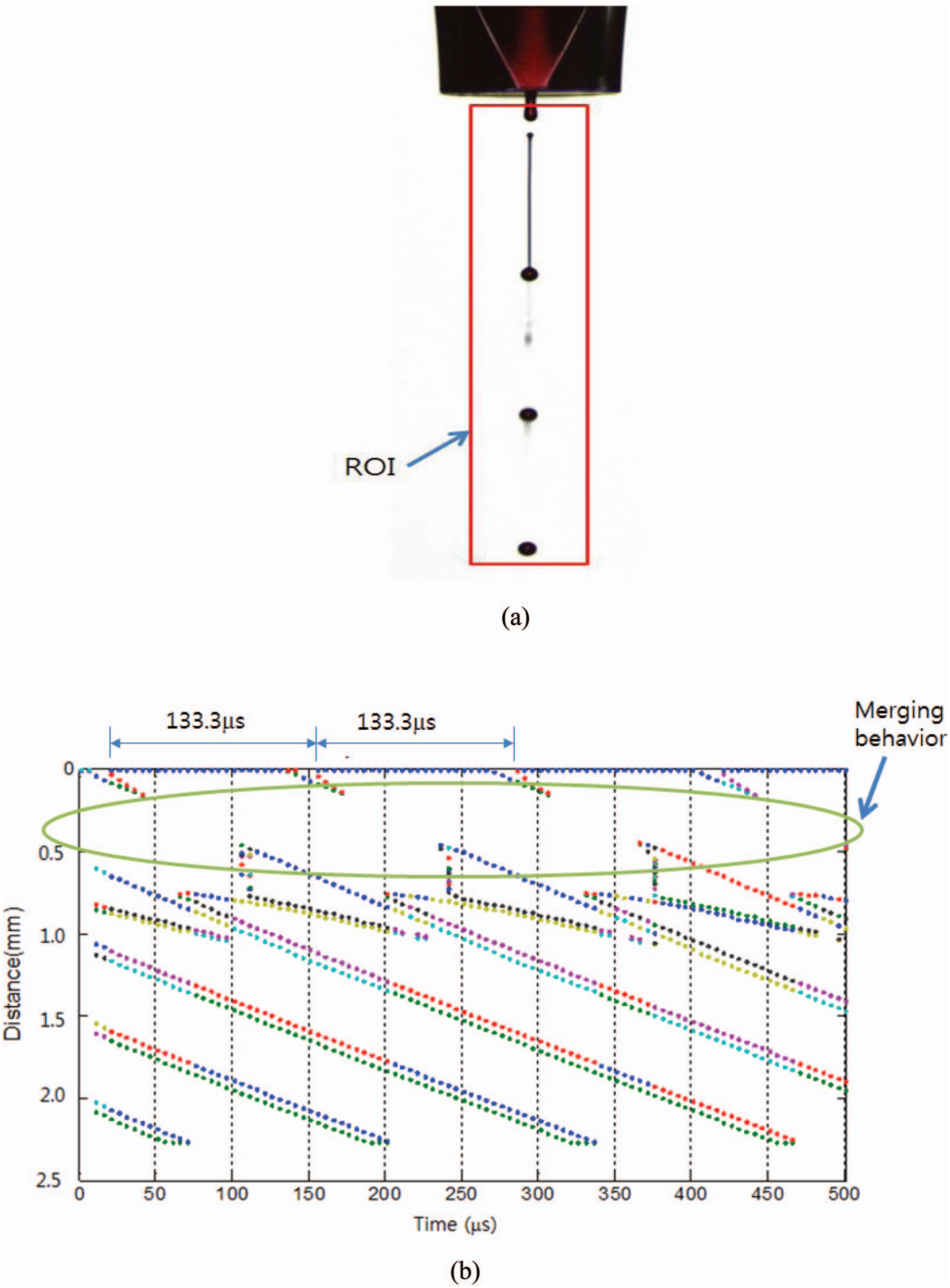

FIG. 8. Drop formation measurement using fixed ROI (7.5 kHz jetting). (a) Fixed ROI. (b) Drop formation curve.

(2) Stage 2: Single tracked droplet

When the initial extruded droplet of interest is detected using the edge detection described in Fig. 6, the droplet location is tracked by a tracking algorithm in each sequential image. From the tracked droplet, the size and location of ROI are re-defined such that the lower location of ROI can be defined by the bottom location of the tracked droplet, while the upper limit is fixed at the nozzle surface, as shown in Figs. 9(a) and 9(b). This process continues until the subsequent main droplet appears from the acquired image.

(3) Stage 3: Two tracked droplets

A subsequent droplet will appear from the nozzle after the jetting period (the inverse of the jetting frequency) from the initial extruded droplet detection. The initial subsequent droplet can also be detected by the same edge detection algorithm described earlier. Then, two consecutive main droplets are tracked simultaneously to define the variable ROI.

From two subsequent droplets, the lower and upper boundaries of the variable ROI can be defined by the bottom locations of two tracked droplets as shown in Figs. 10(c)–10(f). To give a better understanding of high frequency jetting

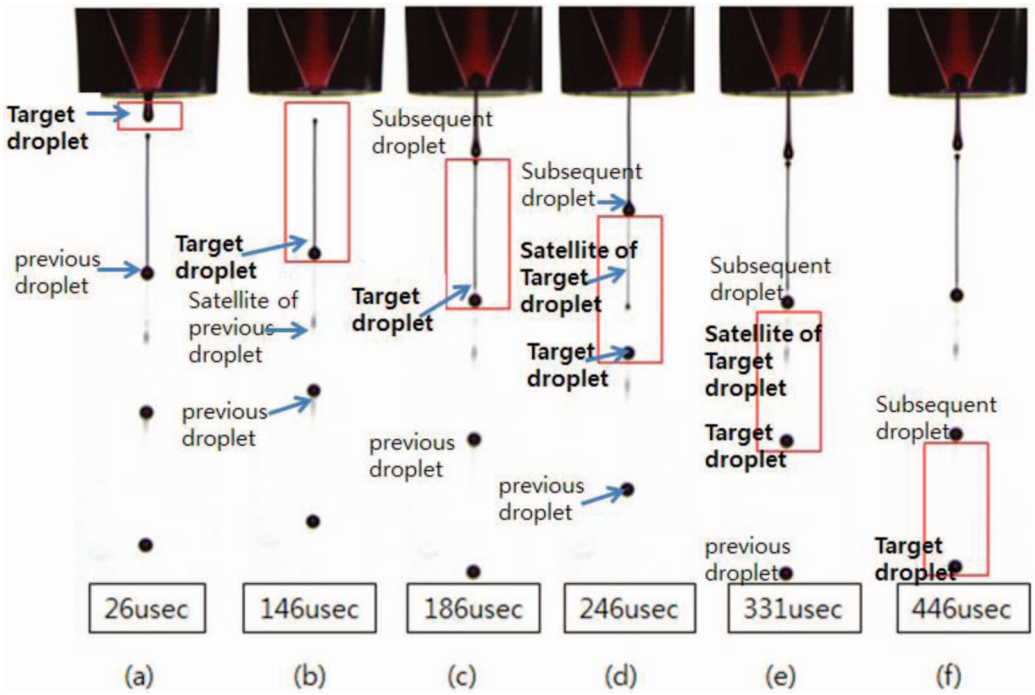

FIG. 9. Variable ROI based on tracking of jetting droplet at 7.5 kHz.

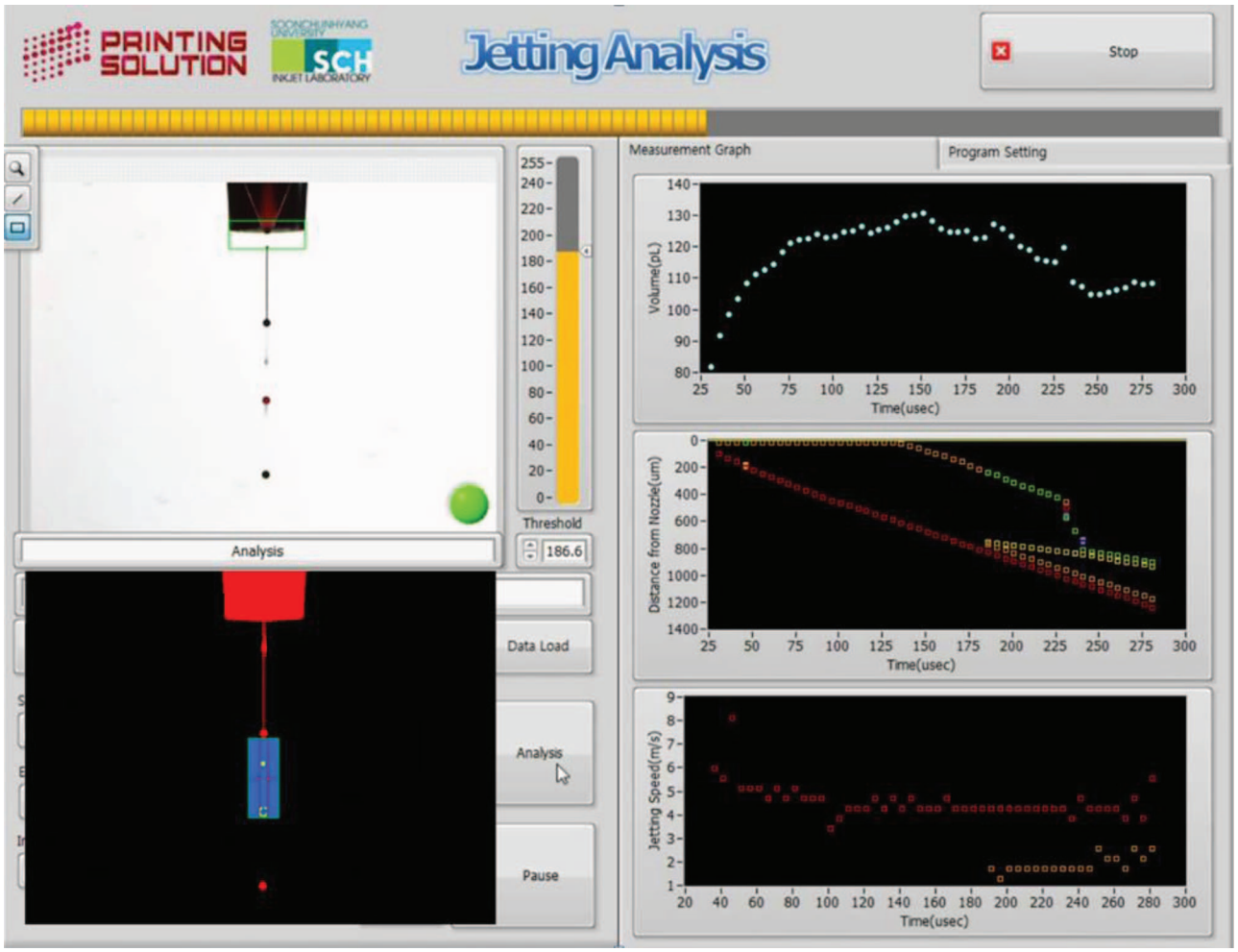

FIG. 10. Laboratory developed software for high frequency jetting measurement. (Multimedia view). [URL: http://dx.doi.org/10.1063/1.4879824.1]

measurement, the laboratory developed software (Multimedia view) is shown in Fig. 10.

C. Drop formation curve

By using the proposed variable ROI, the droplet of interest can be effectively analyzed while excluding image analysis of many other subsequent droplets.

Fig. 11 shows the measured drop formation curve for 7.5 kHz jetting using the variable ROI. The details for obtaining the drop formation curve can be referenced in Ref. 5. Compared to the drop formation measurement using the fixed ROI in Fig. 8(b), the jetting behavior of high-frequency jetting can be clearly understood if the variable ROI is used. However, it should be noted that the droplet of interest could interact with subsequent droplets in high-frequency jetting, which could affect the droplet volume and the jetting speed.

In the initial stage, the initial jetted droplet could interact with the ligament of a previous droplet at the bottom boundary of the ROI (0–110 μs) Later, the long ligament in contact with the upper limit of the ROI interacts with subsequent droplets (130–250 μs). Figs. 9(c) and 9(d) show images at 186 and 246 μs when a long ligament is in contact with the upper limit of the ROI. These interactions are dominant in the beginning and become less significant during drop formation.

D. Jetting speed curve

There seems to be no standardized method for jetting speed measurement, and the measured results might differ according to the measurement location. The measurement method needs to be generalized, and includes the case of droplets with ligaments and satellites, since long ligaments and satellites are likely to occur in most cases.

The jetting speed of the main droplets and satellites with respect to time can be calculated from the drop formation curve.[5] However, if a previous fixed ROI[5] is used, the jetting speed curve will be very complex due to the many other droplets in high-frequency jetting. So, the jetting speed curve based on variable ROI is effective for understanding the jetting behavior of high-frequency jetting, as shown in Fig. 12. This figure shows that that jetting speed can vary during drop formation because of the viscoelastic behavior of the ligament, which is closely related to the change of its shape during the drop formation.[5] Additionally, in high-frequency jetting, the interaction with subsequent droplets may influence the jetting speed.

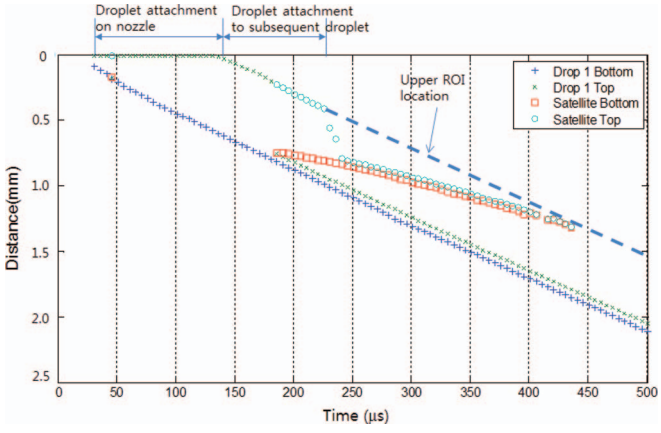

FIG. 11. Drop formation curve of high-frequency jetting (7.5 kHz).

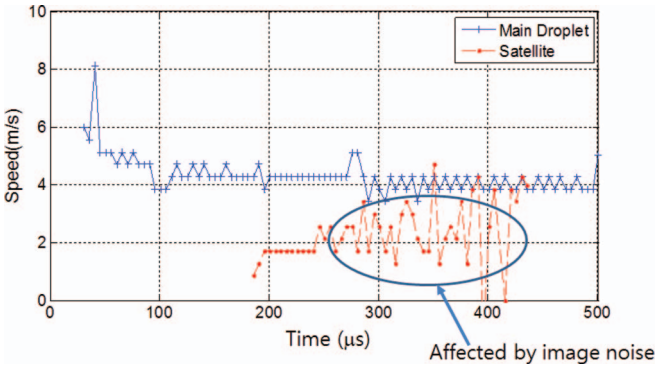

FIG. 12. Instantaneous jetting speed curve of 7.5 kHz jetting.

In the 7.5 kHz jetting shown in Fig. 12, the main droplet jetting speed (4–6 m/s) is higher than the satellite jetting speed (1–2.5 m/s). As a result, the satellite with a long ligament eventually merged with the subsequent droplets at 420 μs.

Note that the measurement of the jetting speed curve is more sensitive to image resolution and image quality. Particularly, the satellite is more affected by such errors because smaller and thinner images are subject to image noise. A camera resolution of 1600 × 1200 was used for measurement, and the zoom lens was adjusted for a pixel resolution of about 2.14 μm per pixel. If a high-magnification lens is used, then only the local behavior along a short travel distance is measured. So, higher-resolution camera is recommended if the measurement quality needs to be increased.

E. Droplet volume measurement

One of the main advantages of the variable ROI is that the droplet volume behavior of the target droplet can be calculated while excluding many other subsequent droplets in the image, as shown in Fig. 13. The edge detection algorithm is used to measure droplet volume. To define a set of horizontal ROI lines, the variable ROI is equally divided in the vertical direction. Then, from each ROI line, edges are detected to calculate the droplet volume. The diameter of each cylinder can be calculated by using the detected edge information, and the droplet volume is the summation of the sliced cylinder volume, as shown in Fig. 13(b).

Similar methods to calculate the droplet volume have been discussed.[2,9] However, the previous methods did not account for droplet measurement in high-frequency jetting and cannot be directly used for close or merged droplets.

Fig. 14 shows the drop volume behavior of 7.5 kHz jetting measured using the variable ROI. The interactions among subsequent droplets can be understood from the measured volume with respect to time. The measured volume changes continuously until the droplets are totally detached from the nozzle and the interaction among subsequent droplets diminishes. As a result, the measured volume can differ according to the measurement time and location, so the measurement standardization is needed. From the droplet volume behavior

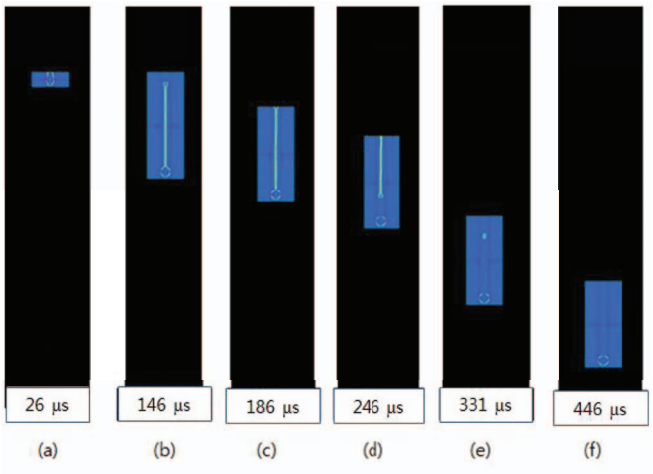

(a)

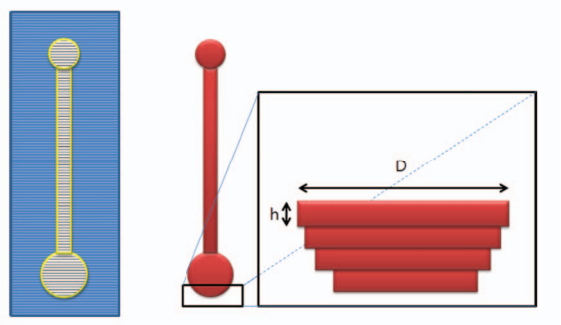

(b)

FIG. 13. Image processing algorithm for droplet volume measurement. (a) Droplet volume measurement using variable ROI (7.5 kHz). (b) Droplet volume calculation algorithm.

with respect to time, we can judge the proper measurement location from the droplet volume where the exact droplet volume per single jetting trigger can be measured.

1. Beginning stage (0–150 μs)

In the beginning, there is a volume increase until 150 μs because the droplet is being developed from the nozzle with the ROI size increasing. In addition, in this particular case, the ligament of previous droplets may be attached to the droplet of interest in the initial stage. The ligament or satellite of a previous droplet is slower than the main droplet at 7.5 kHz. As a result, the ligament (or satellite) will be merged with the droplet of interest, resulting in an additional increase in droplet volume in the beginning stage.

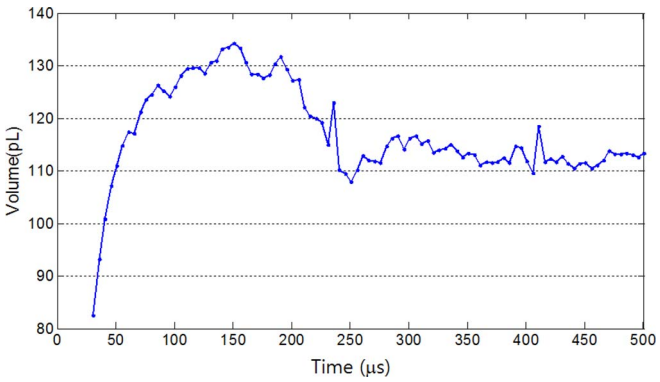

FIG. 14. Droplet volume behavior during drop formation.

2. Interaction with subsequent droplet (150–240 μs)

The next droplet may appear after 133 μs from extrusion of the droplet of interest at 7.5 kHz. Even in such a case, the ligament of the current droplet may not be pinched off from the nozzle. Due to the slower speed of the upper ligament, the droplet volume of interest decreases from 130 pL to 110 pL because a portion of the ligament is lost by adding droplet volume to the subsequent droplet.

3. Droplet volume measurement time and location (240 μs)

Finally, most slow ligaments are merged with subsequent droplets at 240 μs, when the droplet volume does not change significantly. We can determine the corresponding location from the nozzle surface to be about 1.5 mm from Fig. 11. The measured droplet volume per single trigger is about 110 pL. In this way, the droplet volume per single trigger can be measured in high-frequency jetting.

III. FREQUENCY SWEEPING OF JETTING PERFORMANCE VIA TRACKING ALGORITHM

A. Frequency sweeping of jetting speed

To understand the jetting performance with respect to jetting frequency, a frequency sweep of the jetting speed is commonly used. However, few published studies have discussed automatic measurement algorithms for frequency sweeping of the jetting performance.

An automatic frequency sweeping method for jetting speed as well as droplet volume can be difficult to implement due to the complexity if drop formation with satellites and ligaments is considered. To simplify the measurement of jet speed variation and droplet volume variation with respect to jet frequency, we propose an effective frequency sweep method, from a printing point of view based on the tracking method. The use of a tracking algorithm is advantageous because it can be applied to both low-frequency jetting and high-frequency jetting measurement.

1. Previous jetting speed measurement methods

To the best of our knowledge, two different jetting speed measurement methods have been used according to jetting frequency.

- Jetting speed measurement for low-frequency jetting
  The jetting speed can be obtained by locations of droplets from two images taken at two pre-determined timings of LED lights, T1 and T2,[3]

$$V = \frac{D2 - D1}{T2 - T1}, \quad (1)$$

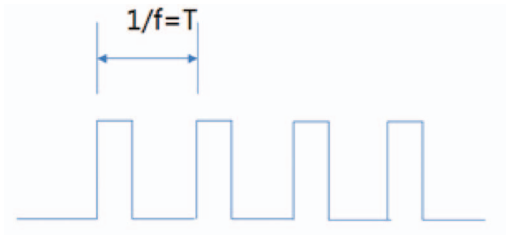

(a)

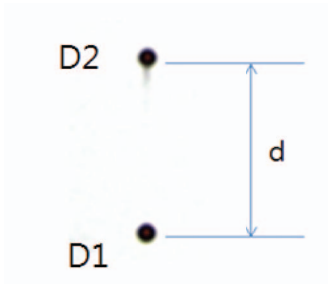

(b)

FIG. 15. Jetting speed measurement for high-frequency jetting. (a) Jetting trigger pulse. (b) Consecutive droplets due to high-frequency jetting.

where D2 is the droplet location at T2, while D1 is the droplet location of T1.

- Jetting speed measurement for high-frequency jetting
  In high-frequency jetting, many subsequent droplets are likely to appear on the image since the jetting trigger interval (T) becomes short. Most inkjet companies seem to use a single image rather than two images taken from different timings, as shown in Fig. 15. Then, the measurement of jetting speed is based on the distance between any two consecutive droplets that appear in a single image as follows:

$$V = d * f = d/T, \tag{2}$$

where f is the jetting frequency in Hz, and d is the distance between two subsequent droplet locations, D1 and D2. T (the inverse of f) is equal to the time required for the droplet at position D2 to travel to position D1. The distance between droplets is likely to be smaller as the frequency increases.

There are two difficulties in measuring high-frequency jetting speed based on a single image. First, the measured location of droplets, D1 and D2, should be that of the main droplets produced by each trigger pulse for jetting. If satellites exist, the satellite droplets should be excluded from image analysis to measure the travel distance of main droplets between two jetting triggers. Second, most previous measurement methods are based on the spherical droplets, so that measurement location should differ according to jetting conditions. Note that droplets tend to be spherical during the drop formation process, and a long travel distance may be needed to make sure that the droplets become spherical. However, the measured jetting speed more than 1 mm from the nozzle may not be of interests from a printing point of view. The stand-off distance, which is the distance between the nozzle and the substrate, is normally less than 1 mm to reduce the placement errors during the printing process. To evaluate the jetting speed from a printing view point, the jetting speed at the point of the target substrate should be used rather than that at an arbitrary location where the droplet becomes spherical.

2. Frequency sweep method for high-frequency jetting

To measure the jetting speed for the purpose of frequency sweeping, we propose two different methods: (1) using the instantaneous jetting speed, Vi, at the location of the target substrate, and (2) using the average jetting speed, Va, from that of the jetting trigger to the time of reaching the target location. For both methods, a fixed measurement location at the stand-off distance, S, is used as shown in Fig. 16.

a. Instantaneous jetting speed at target location The instantaneous jetting speed at the target location might be related to the droplet impact and spreading behavior on the target location. The instantaneous jetting speed at the target location can be calculated using Eq. (1) with short timing, T2-T1. In most previous methods, two fixed timings of T2 and T1 are used for jetting measurement.[3,4] In such cases, the measured droplet location at fixed T2 or T1 may differ according to frequency. However, the proposed method uses a fixed target location and the times of T2 and T1 should differ according to the drop formation. To obtain T2 and T1 for two droplet images, we need to obtain Ta, which is the time when the droplet reaches its target location. In the case of low frequency jetting, the trigger delay time of a strobe LED light can be adjusted in

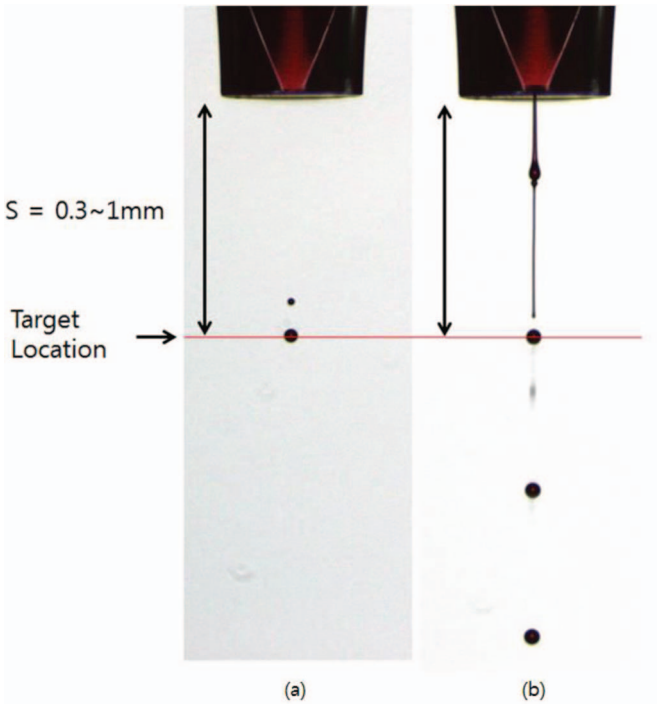

FIG. 16. Target location for jetting speed measurement. (a) Low frequency jetting. (b) High frequency jetting.

order to find Ta, either manually or automatically via tracking algorithm. However, in the case of high frequency jetting, it is necessary to use the proposed tracking algorithm to find the target droplet among many other subsequent droplets. In this way, the trigger delay time of a strobe LED light, i.e., Ta, can be automatically searched for when the target droplet reaches the substrate location. Then, we can set T1 = Ta and T2 = T1+Δt. If Δt is too short, the jetting speed error due to image quality will be amplified. If Δt becomes large, the long-term average jetting speed is obtained rather than the instantaneous jetting speed at the target location. Considering this trade-off relationship, Δt is set to 20 μs in this study.

The tracking algorithm requires sequential images to find ta by tracking the target object location. So, many sequential images need to be scanned for each frequency. To obtain the frequency sweep of the jetting speed, it might take a longer time than the method based on fixed times of T2 and T1.

b. Average jetting speed at target location Unlike the instantaneous jetting speed, the average jetting speed requires only a single time, ta, which is obtained by the tracking algorithm. The average jetting speed can be written as

$$\mathrm{Va} = \mathrm{S}/\mathrm{Ta}. \tag{3}$$

The average jetting speed, which is measured at the target location (the stand-off distance from the nozzle) can be useful to evaluate printing accuracy. If patterns for printing are complex, the actual jetting frequency is not a single fixed frequency and varies significantly during printing. Therefore, the jetting speed, Va, from a droplet nozzle could be more affected during the printing process compared to that with a low-frequency nominal jetting speed (Vn).

The placement errors due to frequency jetting variation can be calculated by the time variation (Δt_a) for an ink droplet to reach the substrate and printing speed (Ps) as

$$\mathrm{Error} = \Delta t_a * \mathrm{Ps}, \tag{4}$$

where the time variation, Δt_a, from nominal t_a, can be written as

$$\Delta t_a = \mathrm{Tn} - \mathrm{Ta} = \frac{S}{Vn} - \frac{S}{Va} = \frac{(Va - Vn)}{VnVa} S. \tag{5}$$

Tn, S, and Vn are the nominal time of low-frequency jetting required to reach the substrate for a jetting signal, the stand-off distance, and the nominal jetting speed, respectively.

To reduce the placement error, a short stand-off distance, S, is recommended to reduce the placement error, as shown in Eqs. (4) and (5). However, if the distance is too short, there is a possibility of mechanical contact between the inkjet head and substrate. A low printing speed, Ps, can reduce the placement errors, as shown in Eq. (4). However, high-printing speed is recommended to increase the productivity as a manufacturing tool. As a result, the jetting speed variation due to jet frequency, Va-Vn, should be minimized to ensure accurate droplet placement. The method for suppressing the jet speed variation to measure jet accuracy is beyond the scope of this work and needs further investigation. The method to design a waveform for suppressing residual pressure waves, which affect jet speed variation, has been discussed in Ref. 6.

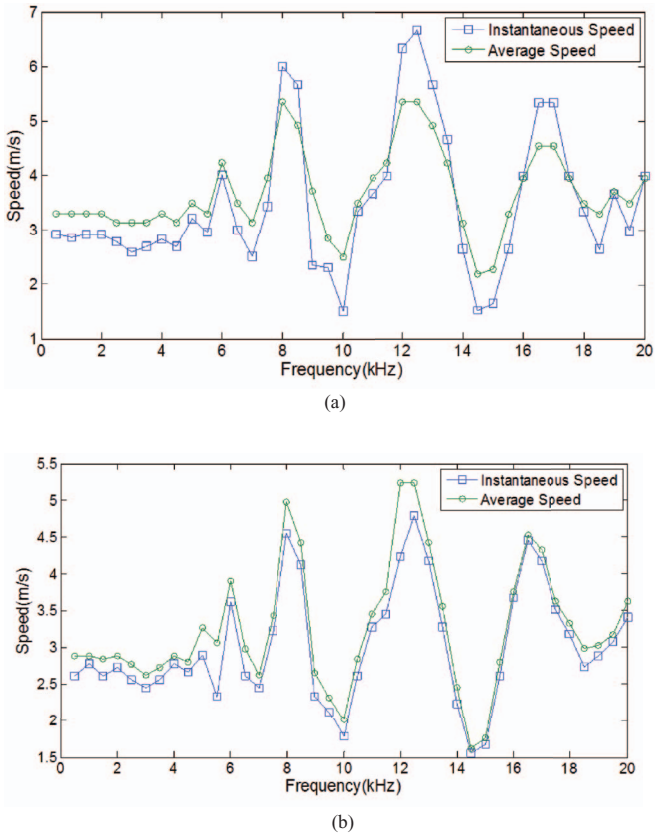

FIG. 17. Frequency sweep of jetting speed. (a) Measured result at 0.3 mm. (b) Measured result at 1 mm.

Fig. 17 shows the experimental results of the frequency sweep of the jetting speed with the jetting speed variation according to jet frequency. The frequency scan of the jetting speed is based on Eqs. (1) and (3) at the target location. The jetting speed could vary by up to 100% compared to the nominal jetting speed, depending on the jetting frequency. Two different target locations of 0.3 mm (Fig. 17(a)) and 1 mm (Fig. 17(b)) were used for jetting speed measurement. The overall jet behavior looks similar to periodic behavior according to the jet frequency. Note that the measured jetting speed differs by about 10%–20% according to measurement techniques or measurement location. If evaluation of the jet speed variation is required for the purpose of comparison, measurement standardization is required.

The jetting speed of the satellite droplets is not included in the frequency sweep shown in Fig. 17 due to complexity, because satellites may not exist, or the number of satellites can differ according to jet frequency.

B. Frequency sweep of droplet volume

In high-frequency jetting, the droplet volume measurement is much more difficult, because the satellites or ligaments might merge with subsequent droplets. In Sec. III A, we recommended that the jetting speed be measured at the target location of the substrate. However, the droplet volume

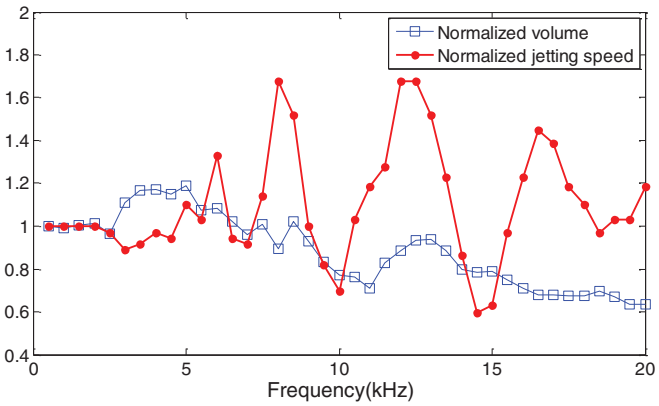

FIG. 18. Frequency sweep of normalized jetting speed and droplet volume.

should be measured at a sufficiently low location from the nozzle surface, because the interaction among droplets could be dominant in the beginning.

The interaction may not vanish completely at the target (substrate) location of 1 mm. For example, in case of 7.5 kHz jetting, the droplet merging behavior completed at 246 μs, which corresponds to 1.5 mm from the nozzle. The interaction behavior differs according to the jetting frequency and other jetting conditions. As a result, the measurement location for droplet volume could differ according to jetting frequency. The droplet volume with respect to time in Fig. 14 can be used to obtain the frequency sweep for the droplet volume. The droplet volume is selected at the time when the drop volume does not vary significantly with respect to time to obtain the droplet volume for the frequency sweep. Alternatively, to obtain the frequency scan of the droplet volume, a measurement location that is sufficiently far from the nozzle, such as 2 mm, where the droplet interaction effect might vanish, can be used as a fixed measurement location.

Fig. 18 shows the normalized frequency sweep results of the droplet volume for comparison with the normalized jetting speed. It is well known that the increase in droplet volume is proportional to the jetting speed[2] if the driving voltage amplitude increases. However, unlike the increase in voltage amplitude, the jetting speed is not always proportional to the droplet volume if the jetting speed variation is caused by the jet frequency. As shown in Fig. 18, it can be clearly understood that the jetting speed variation has periodic behavior according to the jetting frequency due to the pressure wave inside the head having periodic behavior.[6,10] However, the droplet volume tends to be reduced as the frequency increases. One possible reason for which there may be droplet volume decrease in high frequency jetting is due to incomplete ink re-fill in the inkjet head. Further research is required to understand the relationship between the droplet volume and jetting speed in high-frequency jetting.

IV. CONCLUSIONS

The measurement of high-frequency jetting behavior is complex, because many of subsequent droplets appear in the measured images. To simplify the measurement of high-frequency jetting, a particle tracking algorithm was applied. Two different inkjet measurement methods based on a tracking algorithm were discussed in this study: (1) drop formation; (2) frequency sweep of the jetting speed and droplet volume.

Based on the tracked droplets, we proposed a variable ROI, of which the location and size are re-defined in each sequential image, to focus on jetting behavior (drop formation) of the target droplet while excluding other droplets. By using the variable ROI, the droplet volume with respect to time can be measured and it was shown to be effective for evaluating interactions among subsequent droplets due to close droplet locations.

The tracking algorithm was also used to obtain the required time for a droplet to reach the target location. In this way, the jetting speed measurement location can be fixed to the target location, where the substrate for printing is located. The use of a fixed location for the jetting speed measurement has advantages over jetting measurement at a fixed time from a printing point of view.

Finally, frequency sweep methods for the jetting speed and droplet volume were proposed. From the frequency sweeping results, we found that the increases (or decreases) in jetting speed are not always proportional to the droplet volume if the jetting frequency accounts for jetting speed variation. Further study is needed to investigate the relationship between droplet volume and jetting speed when the frequency increases.

ACKNOWLEDGMENTS

This work was supported by Mid-career Research Program through a NRF grant funded by the MEST (NRF-2013R1A2A2A01004802) and was partially supported by the Soonchunhyang University Research Fund.

[1]K. S. Kwon and W. Kim, "A waveform design method for high speed Piezo inkjet printing based on self-sensing measurement," Sens. Actuators, A **140**, 75–83 (2007).
[2]K.-S. Kwon, "Vision monitoring," in *Inkjet-Based Micromanufacturing*, edited by J. G. Korvink, P. J. Smith, and D.-Y. Shin (Wiley-VCH Verlag GmbH & Co. KGaA, Weinheim, Germany, 2012).
[3]K. S. Kwon, "Speed measurement of ink droplet by using edge detection techniques," Measurement **42**(1), 44–50 (2009).
[4]Y. Kipman, "Three methods of measuring velocity of drops in flight using jetxper," in *Proceedings of NIP25 and Digital Fabrication, September 20–24, Kentucky* (Society for Imaging Science and Technology, 2009), pp. 71–74.
[5]K. S. Kwon, "Experimental analysis of waveform effects on satellite and ligament behavior via in situ measurement of the drop-on-demand drop formation curve and the instantaneous jetting speed curve," J. Micromech. Microeng. **20**, 115005 (2010).
[6]K. S. Kwon, "Waveform design methods for piezo inkjet dispensers based on measured meniscus motion," IEEE/ASME J. Microelectromech. Syst. **18**(5), 1118–1125 (2009).
[7]H. Dong and W. W. Carr, "An experimental study of drop-on-demand drop formation," Phys. Fluids **18**, 072102 (2006).
[8]H. Dong, W. W. Carr, and J. F. Morris, "Visualization of drop-on-demand inkjet: Drop formation and deposition," Rev. Sci. Instrum. **77**, 085101 (2006).
[9]I. M. Hutchings, G. D. Martin, and S. D. Hoath, "High speed imaging and analysis of Jet and drop formation," J. Imaging Sci. Technol. **51**, 438–444 (2007).
[10]D. B. Bogy and F. E. Talke, "Experimental and theoretical study of wave propagation phenomena in drop-on-demand ink jet devices," IBM J. Res. Develop. **28**(3), 314–321 (1984).